A circadian transcriptional sub-network and *EARLY FLOWERING 3* control timing of senescence and grain nutrition in bread wheat

Christopher R. Buckley[1], Joshua M. Boyte[1], Robert L. Albiston[1], Jessica Hyles[2], Jesse Beasley[1], Alexander AT Johnson[1], Ben Trevaskis[2], Alexandre Fournier-Level[1], Michael J. Haydon[1] *

[1]School of BioSciences, University of Melbourne, Parkville, VIC 3010, Australia

[2]CSIRO Agriculture and Food, GPO Box 1700, Canberra, ACT 2601, Australia

* Corresponding author: m.haydon@unimelb.edu.au

Abstract

Circadian clocks control daily and seasonal timing of physiology and development. Because of their influence on photoperiodic flowering, variants in circadian clock genes have been selected for phenology during domestication of cereal crops. To explore the potential impact of this genetic variation on circadian-regulated traits, we investigated the relationship of the circadian clock and leaf senescence in hexaploid bread wheat. Phenotyping of a collection of elite wheat cultivars identified significant variation in circadian rhythms which was associated with timing of senescence and nutrient mobilisation efficiency. RNA sequencing revealed substantial reorganisation of the circadian-regulated transcriptome during senescence and a transcriptional sub-network representing a link between the circadian oscillator and regulators of leaf senescence. We used genotypes of multiple circadian clock genes to assign cultivars to 'chronotypes', which could be used to predict circadian-regulated phenotypes. This identified a deletion variant of *EARLY FLOWERING 3-D1 (ELF3-D1)* attributed to a phenology locus, *Earliness per se (Eps-D1),* and we used near-isogenic lines (NILs) to show that it affects timing of senescence and grain protein content (GPC). Thus, there are potential consequences of circadian clock genes selected for phenology on other valuable crop traits.

Keywords

Triticum aestivum, circadian clock, leaf senescence, GPC, chronotype

Introduction

Leaf senescence is a controlled process involving the degradation of chlorophyll, downregulation of photosynthesis and the transport of remobilised nutrients to nascent tissues[1]. Efficient mobilisation of nutrients from vegetative to reproductive tissues during leaf senescence is a key determinant of plant fitness. The relative timing of senescence affects a trade-off between resource accumulation and usage[2] and can be adjusted to balance these processes for adaptation to different environments[3–5]. In cereal crops, the timing of senescence has a major impact on yield traits. In bread wheat (*Triticum aestivum*), high grain protein content (GPC) is a valuable trait which can be achieved with earlier senescence, but typically comes at a cost of lower yield[6]. However, these relationships can be environment-dependent[7–9]. Increasing nutrient content without yield loss across multiple environments is a priority target for crop breeding.

The circadian clock is a biological timing mechanism, comprised of a highly influential gene regulatory network that functions to synchronise development and physiology with daily and seasonal environmental cycles. Plant circadian clocks heavily influence metabolism, transport and signalling underlying growth and development[10]. In numerous cereal crops, the role of the circadian clock in photoperiodic flowering has led to widespread selection of circadian clock gene variants[11]. However, the impact of these variants on other circadian-controlled traits has not been explored.

Since the circadian clock influences timing of senescence in *Arabidopsis thaliana*[12–14], we sought to explore the role of the circadian clock in wheat in controlling leaf senescence and determining grain nutrient content. We compiled a panel of 25 wheat cultivars and found these traits covaried with phenotypic and genotypic variation in the circadian clock. We compared the circadian transcriptomes of mature and senescent flag leaves and used genotypic information for circadian clock genes to define chronotypes within the wheat panel. These suggested a role for the clock gene *EARLY FLOWERING 3-D1* (*ELF3-D1*) and using near isogenic lines (NILs) of a widespread deletion variant in *ELF3-D1,* we found a functional contribution to timing of senescence and GPC.

Results

Circadian period and timing of senescence covary in Australian wheat cultivars

Since the circadian clock influences leaf senescence in Arabidopsis [13–15] and the pace of circadian rhythms shortens with age [16,17], we investigated the relationship between phenotypic variation of circadian rhythms in wheat and the timing of senescence. Using delayed leaf fluorescence (DF) (Fig. 1A), we first measured circadian rhythms in the second leaf of three wheat cultivars 14 days after sowing (DAS; seedling), 33 DAS (5-leaf stage) and 44 DAS (end of tillering). Relative amplitude error (RAE; a proxy for rhythm robustness) did not significantly differ by leaf age (Fig. 1B), but circadian period was significantly shorter in leaves of older plants (Fig. 1C). This demonstrates that changes occur in the circadian clock of wheat plants during ageing.

To assess the extent of phenotypic variation of circadian rhythms in wheat, we chose 15 elite cultivars grown across diverse environments of Australia and measured circadian rhythms of DF in glasshouse-grown plants in two years. Significant differences in mean circadian period were detected between cultivars in each year (Fig. 1D, Supplementary Fig. 1A). In year 1, mean circadian period differed by over four hours over the panel (Fig. 1D,E). Circadian period was mostly consistent within cultivars over both years, except for Viking and Scout, which might suggest strong gene-by-environment interactions in these cultivars (Supplementary Fig. 1B). Nevertheless, there is robust variation in circadian rhythms within elite wheat germplasm which could influence circadian-regulated agronomic traits.

To measure the timing of senescence in the 15 wheat cultivars, we monitored the decline of chlorophyll content in flag leaves after anthesis. There were significant differences in the timing of senescence between cultivars (Fig. 1F), with a maximum mean difference of 10.3 days. We also measured total ion content of mature flag leaves and harvested grain to calculate nutrient mobilisation efficiency. We detected substantial variation in mobilisation efficiency between cultivars (Fig. 1G;) and observed a strongly negative correlation with timing of senescence (Supplementary Fig. 2). Timing of senescence and nutrient mobilisation efficiency were both significantly correlated with circadian period in year one (Fig. 1H,I), such that cultivars with shorter period tend to senesce earlier and exhibit more efficient leaf-to-grain nutrient mobilisation. The relationship of these traits to circadian period was weaker in year two due to a strong year-effect for Scout and Viking. Without these cultivars, a stronger correlation was detected (Supplementary Fig. 1C,D). We also measured total GPC, an important trait which

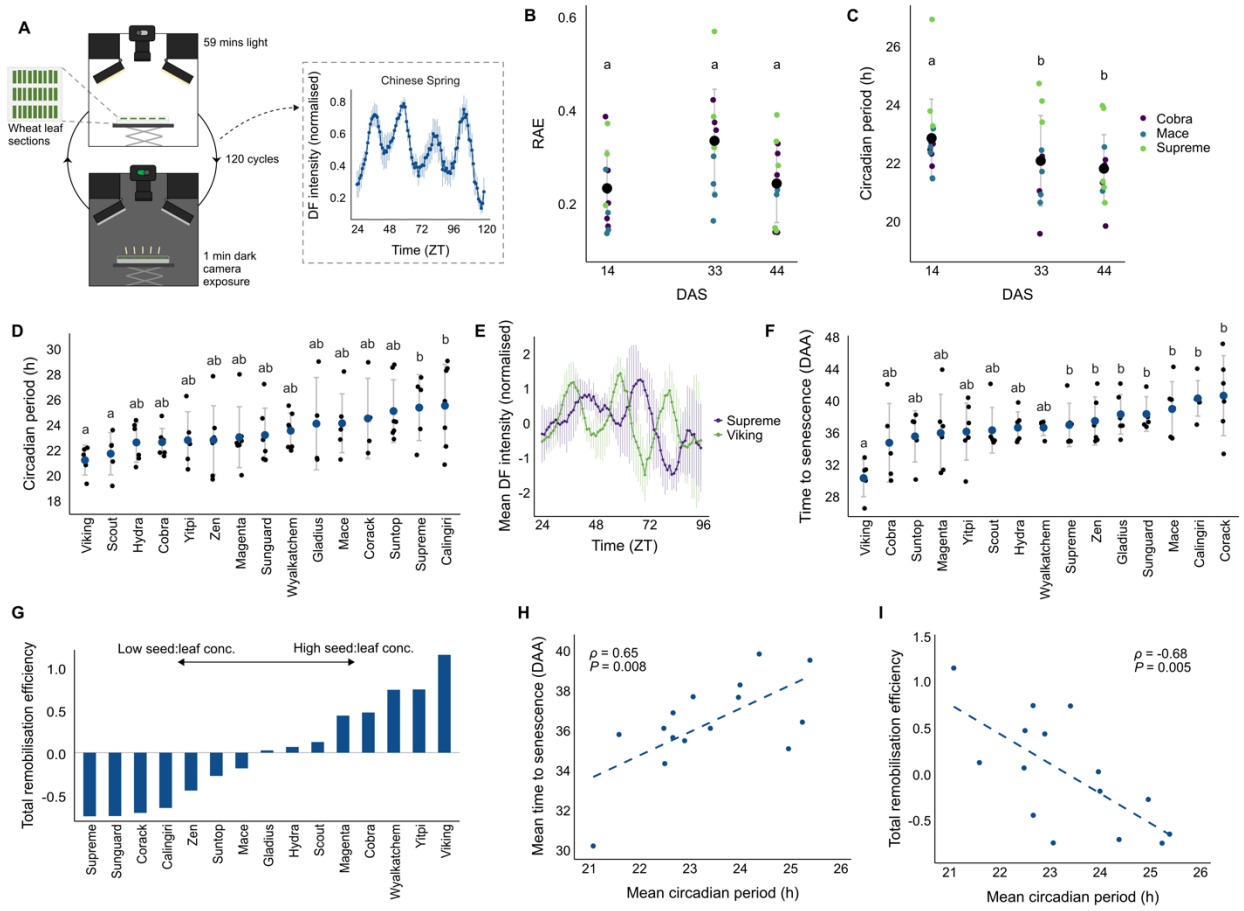

Figure 1: Circadian period of wheat cultivars is associated with senescence and grain nutrition. A, Overview of delayed fluorescence (DF) workflow for measuring wheat circadian rhythms. **B,** Relative amplitude error (RAE) and **C**, circadian period of DF rhythms in 2nd leaf of three cultivars at 14, 33 and 44 days after sowing (DAS). Letters indicate significant differences as determined by one-way ANOVA followed by Tukey's HSD; $P < 0.05$. Error bars represent ±sd, n=15. **D,** Circadian period of DF in 15 Australian wheat cultivars in year one. Letters indicate significant differences as determined by Welch's *t*-test, $P < 0.05$. Error bars represent ±sd, n=8. **E,** Circadian rhythms of DF in the Supreme and Viking. Error bars represent ±sd, n=8. **F,** Time to senescence, (days after anthesis; DAA) in 15 wheat cultivars. Letters indicate significant differences as determined by one-way ANOVA followed by Tukey's HSD; $P < 0.05$. Error bars represent ±sd, n=6. **G,** Total nutrient remobilisation efficiency (ratio of leaf-to-seed nutrient content, see methods) in 15 wheat cultivars. **H**, Mean circadian period (year one) versus mean time to senescence and **I,** total remobilisation efficiency in 15 wheat cultivars. Significance assessed by Pearson's product-moment correlation.

depends on nutrient mobilisation (Supplementary Fig. 3A). GPC was significantly negatively correlated with circadian period in year two, but not year one (Supplementary Fig. 3B,C). Overall, our data suggest strong relationships between circadian period, leaf ageing and senescence, nutrient mobilisation efficiency and GPC in elite wheat cultivars.

115 **Reshaping of the circadian transcriptome during leaf senescence**

116 To explore transcriptional changes in the circadian network during leaf senescence we compared
117 the transcriptomes of mature and senescent flag leaves in *cv.* Mace over 48 h in continuous light
118 (Fig. 2A). Principal component analysis (PCA) separated each individual transcriptome by
119 developmental stage (Supplementary Fig. 4A) and time of day (Supplementary Fig. 4B-E). We
120 used BIO_CYCLE[18] and MetaCycle[19] to detect rhythmic transcripts and estimate their period,
121 phase and amplitude. A total of 11,705 expressed transcripts were called rhythmic in mature flag
122 leaves (15.7% of 74550 expressed) by both algorithms and 16,906 transcripts were rhythmic in
123 senescent flag leaves (22.8% of 74272 expressed) (Fig. 2B). Since fewer rhythmic genes were
124 detected in mature flag leaves compared to senescent flag leaves, the changes in the circadian
125 transcriptome during senescence are unlikely to be due to a general decay in gene expression,
126 we performed gene ontology (GO) enrichment analysis of transcripts that are rhythmic only in
127 senescent flag leaves. Significantly enriched terms included “protein transport”, “peptide
128 metabolic process” and “nitrogen compound transport” (Fig. 2C), suggesting that the circadian
129 network is connected to the reprogramming of metabolism and transport during senescence.
130
131 To identify potential regulators of the circadian transcriptome during leaf senescence, we
132 compared periodicity (BIO_CYCLE’s measure of rhythmicity, from 0 to 1) across families of
133 transcription factors (TFs)[20]. *PSEUDO RESPONSE REGULATORs* (*PRRs*), which are core
134 circadian oscillator genes[21], were the most rhythmic family in both tissue types, followed by
135 Sigma70-like TFs, which regulate rhythmic chloroplast gene expression in Arabidopsis (Fig. 2D)[22].
136 Mean periodicity of the *WRKY* and *CCAAT-HAP2* families was significantly higher in senescent
137 tissue than mature tissue (Fig. 2D). To summarise the overall changes in TF gene expression,
138 we calculated metagene expression values of entire TF gene families (Fig. 2E) and observed a
139 clear increase of *WRKY* metagene rhythmicity during senescence. By contrast, a similar change
140 in rhythmicity was not observed for other TF families with roles in senescence (e.g. *NAC, AP2*
141 and *MYB*[23]). However, we did detect a phase advance of metagenes for the *MYB, PRR* and
142 *Sigma70* families (Fig. 2E). *WRKY* genes are known as regulators of leaf senescence[24] but our
143 data suggests the influence of the circadian clock on their regulation might have been
144 underestimated.
145
146 Among the 8,593 rhythmic transcripts in both tissues, the mean circadian period was ~0.5 h
147 shorter in senescent flag leaves compared to mature flag leaves (Fig. 3A; Supplementary Fig.
148 5B). This is consistent with the expectation for shorter period in older leaves (Fig. 1C). In addition,

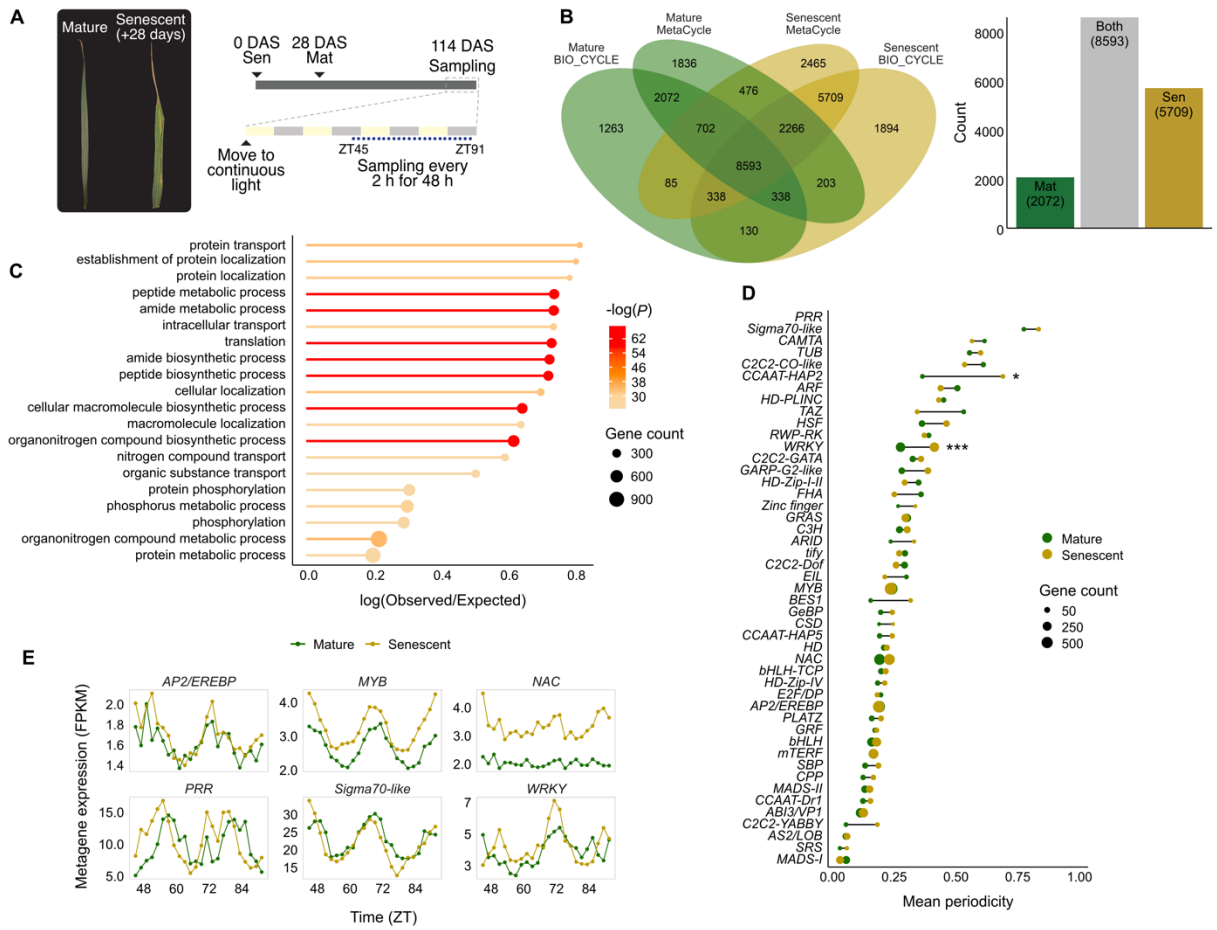

Figure 2: Circadian transcriptional network increases its output at leaf senescence. A, Sampling design of comparative circadian senescence transcriptome. 'Sen' and 'Mat' refer to the sowing dates of plants that were harvested for senescent and mature flag leaves, respectively. **B,** Number of transcripts determined to be rhythmic by BIO_CYCLE[18] and MetaCycle[19]. **C,** Gene ontology term enrichment analysis of transcripts that are uniquely rhythmic in senescent flag leaves. **D,** Comparison of mean periodicity of transcription factor families determined by BIO_CYCLE (0 = arrhythmic). Asterisks indicate significant differences as determined by Welch's *t*-test, * = $P < 0.05$, *** = $P < 0.001$. **E,** Metagene expression (average across entire gene family) of selected transcription factor families.a circadian phase advance of ~0.5 h (corrected for period) was also detected in senescent leaves (Supplementary Fig. 5A,B). Amplitude differences were small between the two developmental stages, although mean amplitude was higher in mature tissue (Supplementary Fig. 5C).

we noted that there was substantial variation in the period differences for individual transcripts outside the global trend (Fig 3A). To identify patterns in differential period, we performed GO term enrichment of transcripts with shorter (< -0.5 h), longer (> 0.5 h) or unchanged (< ±0.5 h) circadian period in senescent leaves. Rhythmic genes with shorter period were significantly enriched for GO categories related to primary metabolism (Fig. 3B,C). Among transcripts with longer period in

168 senescent tissue, terms related to photosynthesis were overrepresented, perhaps reflecting the
169 breakdown of normal rhythmic regulation of photosynthesis (Fig. 3B,C; Supplementary Fig. 3).
170 The two most strongly enriched GO terms within transcripts with unchanged period were “rhythmic
171 process” and “circadian rhythm” (Fig. 3B,C). This suggests that the global shortening of period in
172 the senescent transcriptome could be driven by amplitude or phase changes in the circadian
173 oscillator.
174
175 To identify other transcriptional changes between mature and senescent leaves, we used
176 LimoRhyde[25] to identify differentially expressed (DE) and differentially rhythmic (DR) genes.
177 Among DE genes in senescent leaves, 6,310 upregulated genes were enriched for GO terms for
178 transport and catabolism, and 8,785 downregulated genes were enriched for GO terms related to
179 biosynthesis (Supplementary Fig. 6). There were 1,743 DR genes, enriched for GO terms related
180 to photosynthesis, light signalling and circadian rhythms (Fig. 3D). When we compared DR genes
181 to the remainder of the rhythmic transcriptome, we observed an advanced mean phase in
182 senescent tissue, rather than change in period or amplitude (Fig. 3E).
183
184 **A circadian-regulated sub-network in senescent leaves**
185 We hypothesised that the phase-advanced DR genes, which are enriched for the “circadian
186 rhythm” GO term, represent a sub-network driving changes in the transcriptome. We identified
187 106 TFs among the DR genes, which were characterised by large phase advances
188 (Supplementary Fig. 7A). Several families of TFs were significantly over-represented, including
189 C2C2-Dof, TAZ, FHA, PRR and Sigma70 (Supplementary Fig. 7B). To analyse the interactions
190 between DR TFs, we modelled the putative interactions between members of this gene set using
191 STRING[26]. We identified 308 putative functional and physical interactions, which is 7x more than
192 expected (Hypergeo. test, $P < 1x10^{-16}$). The network includes genes related to hormone signalling,
193 light signalling and photoperiodic flowering, and is centred around core clock genes; *PRRs*,
194 *REVEILLEs* (*RVEs*), *LUX ARRHYTHMO* (*LUX*) and *LATE ELONGATED HYPOCTYL* (*LHY*) (Fig.
195 3F). Evening elements (EEs), which are *cis*-regulatory motifs bound by clock TFs[27], were highly
196 significantly enriched among all DR gene promoters (Supplementary Table 1). These results
197 suggest that there is a circadian-controlled transcriptional subnetwork with advanced phase in
198 senescent tissue.
199

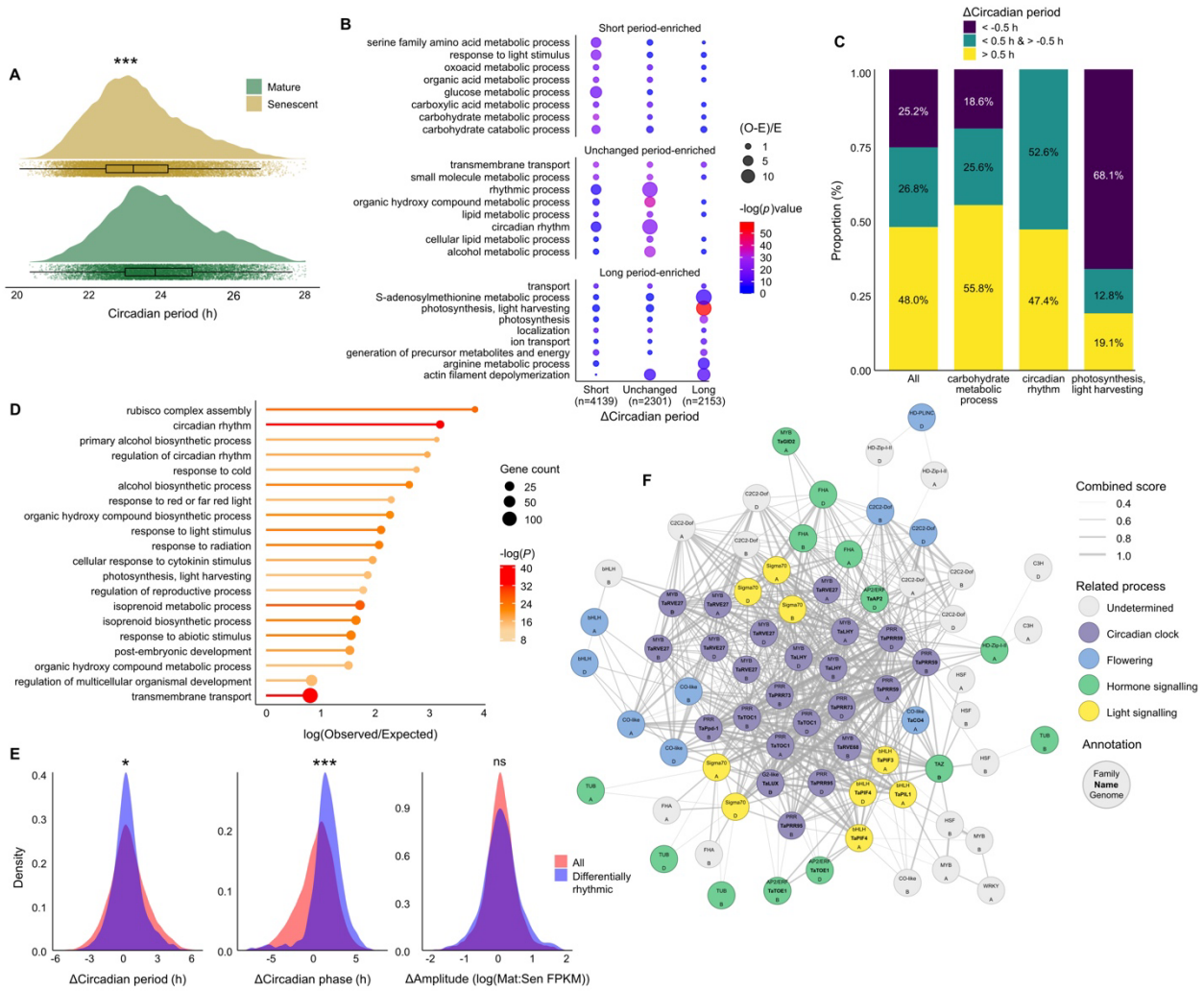

Figure 3: A circadian-regulated transcriptional subnetwork in senescent leaves. A, Distribution of circadian period values of all rhythmic transcripts in mature and senescent flag leaves. Asterisks indicate a significant difference between the mean circadian period values, Welch's *t*-test, $P < 0.001$. **B,** GO term enrichment analysis of transcripts categorised according to the change in circadian period between developmental stages; short period (Δperiod < -0.5 h), long period (Δperiod > 0.5 h), unchanged period (Δperiod < ±0.5 h). O (observed) and E (expected) number of transcripts. **C,** Proportions of transcripts in each Δperiod category for a selection of GO terms. **D,** GO term enrichment analysis of differentially rhythmic (DR) genes. **E,** Distribution of changes in circadian rhythm parameters for DR genes. Asterisks indicate significant differences between DR genes and all other rhythmic genes as determined by Welch's *t*-test, * = $P < 0.05$, *** = $P < 0.001$, ns = not significant. **F,** Putative protein-protein interaction network of DR transcription factors. Combined score reflects the probability of interaction determined by STRING[26]. Related processes are manually assigned after literature and orthology database searches.

We performed a systematic analysis of circadian oscillator gene expression and identified 59 out of 79 putative circadian oscillator genes (Supplementary Table 2) that were rhythmic in both

218 tissues (Supplementary Fig. 8). Mean period difference of this group was 0.52 h, which was similar
219 to the global trend, and suggested that maintenance of period is not uniform across the oscillator
220 (Fig. 3B). Strikingly, the mean phase advance of oscillator genes was 1.37 h, which is significantly
221 larger than the global average (Welch's *t*-test, t (59.5) = 4.21, $P < 0.001$). To categorise the
222 oscillator genes by rhythmic expression patterns, we performed PCA of changes in period, phase
223 and amplitude (Fig. 4A). The three PCs were grouped into six transcript clusters of 1-20 genes
224 by *k*-means (Fig. 4C). Clusters 5 and 6 are mainly comprised of genes expressed around dawn,
225 including *RVEs*, *NIGHT LIGHT–INDUCIBLE AND CLOCK-REGULATED* (*LNKs*) and *LHY* genes
226 (Fig. 4C) and have shorter period in senescing tissue, consistent with the global trend (Fig. 4B,D).
227 Clusters 2, 3 and 4 have advanced phase in senescing tissue (Fig. 4B), similar to the identified
228 subnetwork (Fig. 3F). These are mostly afternoon- or evening-phased genes and include the
229 majority of *PRR* and *LUX* genes (Fig. 4C). Amplitude was increased in cluster 2 genes, and period
230 was unchanged in clusters 2 and 4 (Fig. 4B,D). Thus, there appear to be distinct changes in
231 oscillator genes during senescence according to their phase of expression and this suggests a
232 restructuring of the circadian oscillator during leaf senescence.
233
234 **Identification of chronotypes within elite wheat cultivars**
235 Since the circadian clock appears to strongly influence the wheat transcriptome during leaf
236 senescence, we sought to maximise the circadian gene variation within the wheat panel for further
237 phenotyping. We explored SNP data for the OzWheat diversity panel comprised of 283 Australian
238 cultivars. We found four novel non-synonymous SNPs in conserved regions of clock genes from
239 distinct transcript clusters (Fig. 3C); *TaPRR59-B1* (Cluster 2), *TaLUX-B1* (Cluster 3), *TaTOC1-*
240 *B1* (Cluster 4) and *TaPRR73-A1* (Cluster 6). We used these SNPs and three major polymorphic
241 clock gene loci in wheat (*TaPpd-B1*, *TaPpd-D1* and *TaELF3-D1*[28–30]), to categorise cultivars into
242 six chronotypes (Fig. 5A,B; Supplementary Table 3) and compiled a circadian diversity panel of
243 25 cultivars, representing all six chronotypes (Supplementary Table 4), which were phenotyped
244 for circadian period and timing of senescence (Fig. 5E,F; Supplementary Fig. 9). There were
245 significant differences between chronotypes for both circadian period and time to senescence
246 (Fig. 5C,D). In turn, grain filling was also affected, as thousand grain weight (TGW) differed
247 significantly between chronotypes (Supplementary Fig. 10A,B). However, there were no
248 significant differences between chronotypes for GPC (Supplementary Fig. 10C,D). Although the
249 circadian period values do not correlate with time to senescence and TGW for all chronotypes,
250 chronotype 5 exhibited short period, early senescence and low TGW, while chronotype 6 showed
251 both longer period and later senescence (Fig. 5C,D; Supplementary Fig. 10).

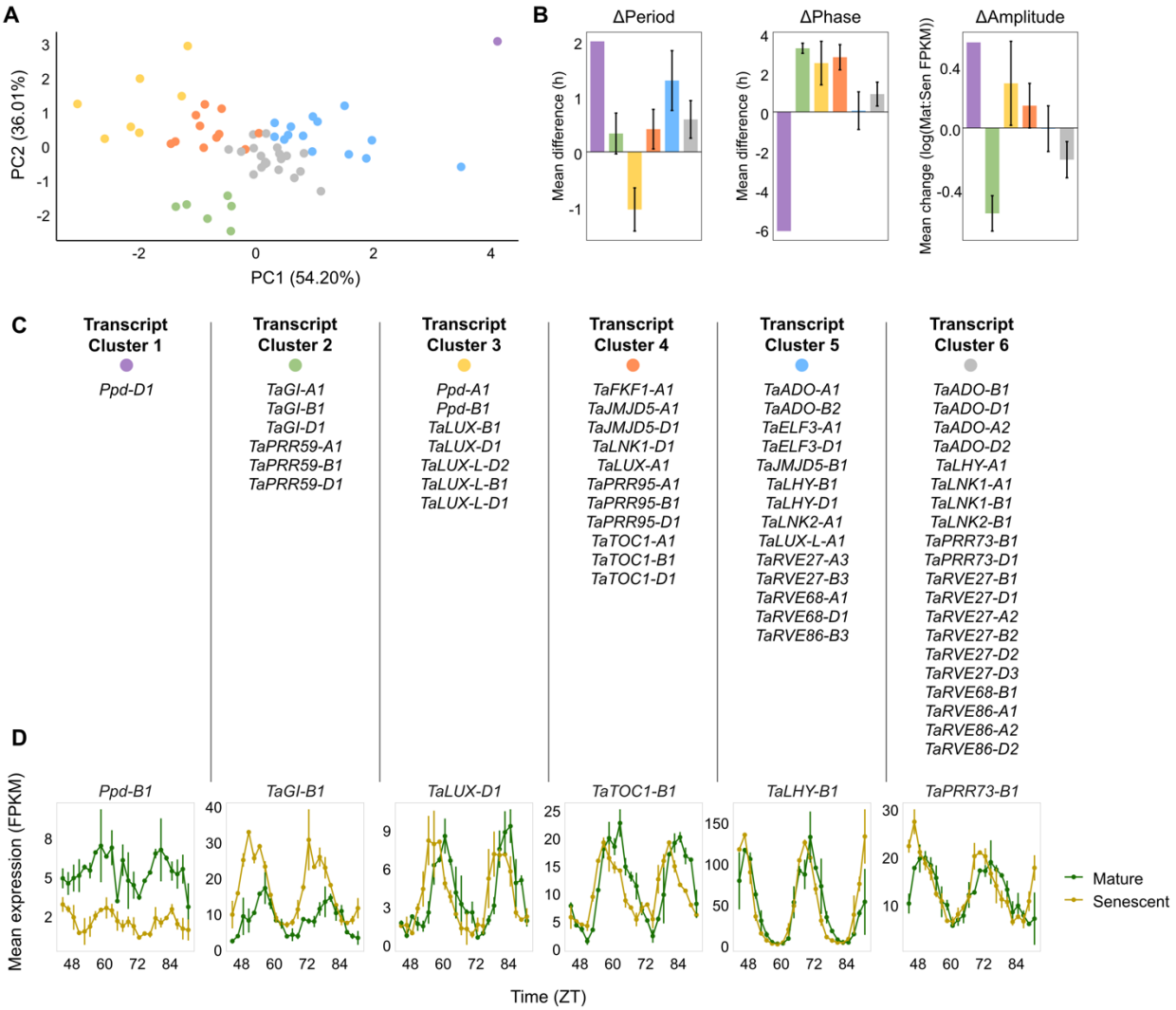

Figure 4: Reshaping of the circadian oscillator during leaf senescence. A, PCA of changes in circadian period, phase and amplitude between mature and senescent leaves for putative circadian oscillator genes. PCs generated were used to group transcripts into 6 clusters (represented by different colours). **B,** Mean change in circadian period, phase and amplitude for each transcript cluster. **C,** Names of genes within each transcript cluster. **D,** Transcript circadian rhythms for a representative gene from each cluster. Error bars represent ±sd.

ELF3-D1 deletion impacts timing of senescence and GPC

Chronotypes 2 and 5 both have a deletion in *TaELF3-D1* and relatively early senescence. To test the potential for this circadian polymorphism on timing of leaf senescence, we used four pairs of near-isogenic lines (NILs) that differ by variation at *TaELF3-D1* (Supplementary Table 3,4). Across the four pairs of NILs circadian period was not significantly different (Fig. 5G,H) and neither was TGW (Fig 5I,J). However, early senescence was detected for the *TaELF3-D1* deletion in three out of four NIL pairs (Fig. 5K,L). Similarly, GPC was reduced by the *TaELF3-D1* deletion in

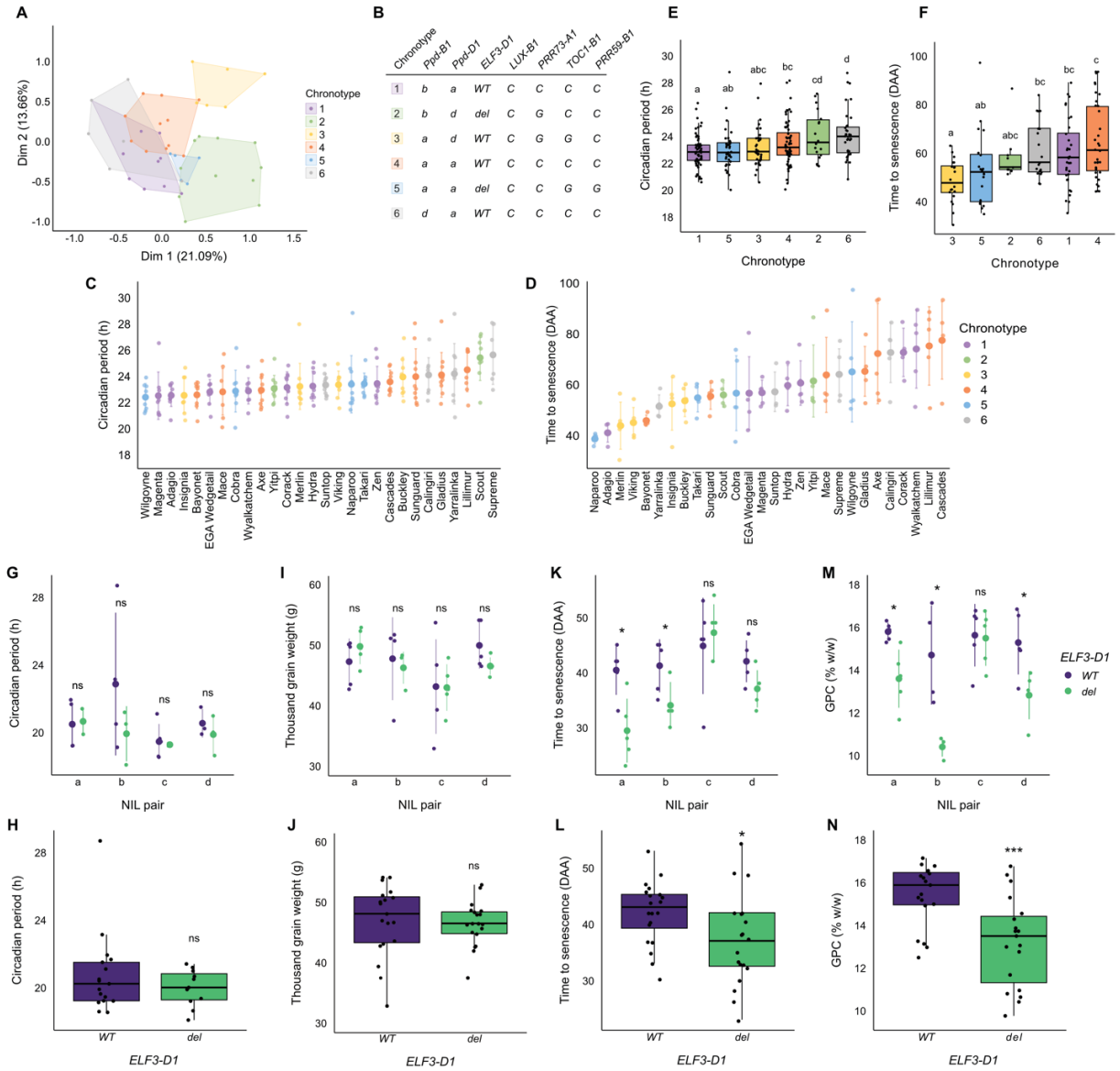

Figure 5: Wheat clock gene variation affects time to senescence and GPC. A, Cultivars from the OzWheat diversity panel were grouped into chronotypes by *k*-modes clustering based on their genotype at seven clock gene markers**.** Multiple correspondence analysis was used to visualise clusters in space. **B,** Mode allelic variation of each cluster (see Supplementary Table 3 for explanation of alleles). **C,** Circadian period (n=10) and **D**, time to senescence (n=5) of 25 wheat cultivars in a circadian diversity panel. Error bars represent ±sd. **E,** Circadian period and **F,** time to senescence for the 25 cultivars by chronotype defined in **A**. Letters indicate significant differences as determined by one-way ANOVA followed by Tukey's HSD; $P < 0.05$. **G,H,** Circadian period, **I,J,** thousand grain weight (TGW), **K,L,** time to senescence and **M,N,** grain protein content (GPC) of near isogenic lines (NILs) for variation at *TaELF3-D1*. Individual NIL pairs are shown in **G,I,K,M.** Error bars represent ±sd, n=5 . Values for all four NILs with functional (*WT*) and *ELF3-D1del (del)* are combined in **H,J,L,N.** Asterisks indicate significant differences between *WT* and *del* alleles as determined by Welch's *t*-test, * = $P < 0.05$, *** = $P < 0.001$, ns = not significant.

282 the same three NIL pairs (Fig. 5M,N). The exception is NIL pair c, which carries a different
283 genotype for *TaPpd-D1* (Supplementary Table 5), a putative downstream target of *ELF3*. Thus,
284 the absence of an effect in this NIL pair could be explained by an epistatic interaction.
285
286 **Discussion**
287
288 We have used a diverse collection of elite wheat cultivars and comparative transcriptomics to
289 explore the influence of the circadian clock on leaf senescence in wheat and assess its impact on
290 grain quality. Our data reveal significant phenotypic variation in circadian rhythms within wheat
291 cultivars and identify strong correlations with timing of leaf senescence, nutrient mobilisation
292 efficiency and GPC. Comparison of the circadian transcriptome in mature and senescent leaves
293 identified a circadian-controlled subnetwork, centred around several core clock genes and
294 connected to possible transcriptional regulators of senescence. Using genotypic information for
295 circadian clock genes in these wheat cultivars we were able to define chronotypes which we show
296 could potentially be used to predict circadian phenotypes and yield traits. Phenotyping of NILs for
297 an extant deletion variant in *TaELF3-D1* revealed a functional contribution of this core circadian
298 clock gene to timing of senescence and GPC.
299
300 ELF3 is a core component of the circadian oscillator as part of the evening complex (EC), a
301 transcriptional repressor complex also comprised of ELF4 and LUX in Arabidopsis[31]. Null mutants
302 in *ELF3* in Arabidopsis and double null mutants in tetraploid wheat have arrhythmic circadian
303 phenotypes[30,32]. Hypomorphic alleles of *elf3* in Arabidopsis have short period phenotypes[33,34].
304 Chronotypes 2 and 5 have a *TaELF3-D1* deletion, and chronotype 5 had a relatively short period
305 (Fig 5). Since we did not detect significant differences between the *TaELF3-D1* NIL pairs, it seems
306 unlikely that this variant alone causes the short period phenotype. Notwithstanding that the
307 *TaELF3-D1* deletion might be recessive to functional A and B homoeologues for circadian period,
308 there are several genotypic differences in clock genes between these two chronotypes, so the
309 short period of chronotype 5 could be due to genetic interactions between different clock alleles.
310 For example, chronotypes 2 and 5 have different alleles at *TaPpd-D1* and *TaPpd-B1*, which are
311 putative regulatory targets of the EC[35].
312
313 We found a significant effect of the *TaELF3-D1* deletion on timing of leaf senescence and GPC
314 for three out of four NIL pairs (Fig 5). This suggests that the widespread *TaELF3-D1* deletion,
315 attributed to *Earliness per se (Eps-D1)* locus[30,36], has a potential negative effect on grain quality,

316 independent of any effect on circadian period. The exception was NIL pair c, which has a promoter
317 deletion within *TaPpd-D1,* in contrast to the functional alleles present in the other three
318 (Supplementary Table 5). Thus, the effect of *TaELF3-D1* on senescence might depend on the
319 genotype at *TaPpd-1.* Notably, *TaPpd-B1* is among the *PRR* genes identified within the
320 transcriptional subnetwork (Fig. 3) which we predict to make a regulatory contribution to leaf
321 senescence.
322
323 Increased GPC is commonly associated with reduced yield in cereal crops[6] and this relationship
324 has been attributed to timing of senescence[2]. TGW, which is an important yield component, was
325 not significantly different between *TaELF3-D1* NILs (Fig 5), but accurate estimates will require
326 multi-year field trials. These will also be required to better assess the robustness of the
327 relationship between circadian period and timing of senescence, since we detected substantial
328 gene-by-environment effects for some cultivars (Supplementary Fig. 1).
329
330 The overall trend in the rhythmic transcriptome was of shorter circadian period in senescent tissue
331 (Fig. 3) which is consistent with expectations of accelerating rhythms with age[16,17] (Fig 1).
332 However, there was substantial variation across the transcriptome. For example, photosynthesis
333 genes had a longer period, which could be explained by general decay in expression and an
334 uncoupling from the core oscillator. Of particular note, genes that were relatively unchanged for
335 period were enriched for circadian genes and instead are characterised by an advanced phase
336 (Fig 3). Indeed, three of the circadian transcript clusters we defined had advanced phase in
337 senescent tissue, and include numerous *PRR* genes, EC genes and *GIGANTEA* (Fig 4). We
338 propose that the phase adjustment of these oscillator genes could be driving the period change
339 of the wider transcriptome. Interestingly, *ELF3* genes and *TaPpd-D1* are among the few oscillator
340 genes that have a substantially shorter period in senescent leaves and might represent a
341 regulatory link between the adjusted oscillator and senescence-regulated genes.
342
343 Our findings have potentially important implications for breeders and growers because they
344 suggest that extant variation in circadian clock genes in crops, which were selected for their
345 effects on phenology, can have a significant impact on other traits such as grain quality. The
346 extent of these effects is likely to depend on genetic interactions between other circadian loci and
347 so identifying chronotypes within wheat germplasm could be a useful tool to predict phenotypic
348 effects. The TFs within the subnetwork are candidates that could be targeted to fine-tune
349 circadian-regulated leaf senescence without affecting the core circadian clock.

350 **Materials and methods**

351

352 **Plant materials**

353 Phenotyping experiments in year one and two used a panel of 15 elite Australian wheat cultivars
354 (Calingiri, Cobra, Corack, Gladius, Hydra, Mace, Magenta, Scout, Sunguard, Suntop, Supreme,
355 Viking, Wyalkatchem, Yitpi and Zen) which were obtained from Australian Grains Genebank
356 (AGG). In the third and fourth years, a 25-cultivar circadian diversity panel was developed by
357 including cultivars from the OzWheat diversity panel developed by the Commonwealth Scientific
358 and Industrial Research Organisation (CSIRO). These additional cultivars were Axe, Bayonet,
359 Buckley, Cascades, EGA Wedgetail, Insignia, Lillimur, Takari, Wilgoyne and Yarralinka.

360

361 Four pairs of NILs with variation at *TaELF3-D1* were derived from a large NIL population with
362 phenology gene variation developed by CSIRO[37,38]. The NILs were generated by crossing donors
363 of phenology genes with the cultivar Sunstate, which carries the *TaELF3-D1del* allele. This was
364 followed by five rounds of recurrent backcrossing to obtain average 97% genetic identity between
365 NILs.

366

367 **Growth conditions**

368 For glasshouse experiments, seeds were sown in July-August (Parkville, Victoria). Growth room
369 and growth cabinet experiments were set to 12 h light (200-280 µmol m^{-2} s^{-1}, 20ºC), 12 h dark
370 (15ºC). In all phenotyping experiments, seeds were chilled at 4°C for 48 h and sown in a mix of
371 sterilised potting soil with 4.5 g/L Osmocote 6-9 month slow-release fertiliser. Full details of growth
372 conditions can be found in Supplementary Note 1.

373

374 **Delayed leaf fluorescence (DF) imaging**

375 Unless specified otherwise, DF was imaged in the second leaves of plants at the 5-leaf stage. In
376 all experiments, 2.5 cm sections were dissected from excised leaves (cut 3 cm from the leaf tip)
377 and placed on 12 cm^2 0.5% agar (type M; Sigma-Aldrich) Petri plates, arranged according to a
378 randomised controlled block design. Leaf sections were imaged using a Retiga LUMO charge-
379 coupled device (CCD) camera (Teledyne Photometrics) fitted with a 25 mm f/0.95 lens housed
380 within light-tight dark boxes. Light (>45 µmol $m^{-2}s^{-1}$) was provided by two LB3 red/blue LED panels
381 (Photek). The lights and camera were controlled by beanshell (bsh) scripts in µManager (version
382 2.0[39]). DF was measured in 120 h of continuous light (LL) conditions by 1 min camera exposure
383 in the dark, following 59 min of light. Camera properties were binning = 4x4, gain = 1, readout

384 rate = 0.650195 MHz 16 bit. DF was measured in leaf sections from image stacks as integrated
385 density using ImageJ (NIH). Timeseries data were uploaded to BioDare2[40] for period analysis of
386 background-subtracted data using the fast Fourier transform non-linear least squares (FFT-NLLS)
387 method[41]. Data were detrended according to the amplitude and baseline detrending method and
388 analysis was performed using a 24 - 96 h window. Estimates of period that fell outside of the
389 range of 24 h ± 5 h or had relative amplitude error (RAE) > 0.6 were excluded. Time series
390 intensity data presented are Z-score normalised.
391
392 **Quantifying time to senescence**
393 Leaf chlorophyll content was recorded using a handheld SPAD meter (Konica Minolta).
394 Measurements were taken three times/week from heading (full emergence of ear). In year two,
395 five SPAD values per plant were measured from the midpoint of the flag leaf of the main tiller and
396 the median value was recorded. In year four, ten SPAD values per plant were measured across
397 the whole flag leaf of the main tiller and the mean value was recorded. Time to senescence was
398 defined as the number of days after anthesis (DAA) to reach 50% of the maximum chlorophyll
399 content. Plants with time to senescence values three standard deviations above or below the
400 overall mean were excluded.
401
402 **Nutrient profiling of grain and leaf samples**
403 Whole flag leaves were harvested at anthesis from six plants of each genotype and mature grains
404 were harvested from another six plants. Flag leaf harvest was performed between 9 am and 12
405 pm (approximately 2-5 h after dawn). For grain samples, all ripened grain heads from each plant
406 were harvested. Thousand grain weight (TGW) was recorded by counting and weighing 50 seeds
407 from each sample. Leaf and grain samples were dried at 65°C for 7 days. Threshed grain samples
408 were sieved with a 2 mm slotted sieve and then milled with a Tube Mill 'Control' (Ika). Each sample
409 was ground for 90 seconds at 25,000 rpm. Dried leaf samples were milled using a TissueLyser
410 (Qiagen), with each sample milled for 2 min at 21.5 Hz with a single 18 mm stainless steel ball
411 bearing. Powdered leaf and grain samples were digested in HNO_3 and ion concentration was
412 determined by inductively coupled plasma optical emission spectroscopy (ICP-OES). Total
413 remobilisation efficiency was calculated as the mean normalised ratio of seed-to-leaf
414 concentration across eight elements (P, S, K, Ca, Mg, Fe, Zn, Mn). Total protein of grain samples
415 was extracted following the protocol of Dupont *et al.*[42] and quantified by bicinchoninic acid (BCA)
416 assay.
417

418 **Defining chronotypes**

419 Clock gene markers were identified by searching for SNPs in the OzWheat diversity panel[43].
420 Genotyping of the entire OzWheat panel has been performed with allele-specific markers for
421 agronomically important genes for phenology (e.g. *Ppd-1* and *ELF3*) and around 26K SNPs were
422 identified by transcriptome sequencing (crown tissue from seedlings) of the panel. The OzWheat
423 polymorphism database was filtered against a set of putative wheat clock genes (Supplementary
424 Table 1), and novel non-synonymous SNPs in clock genes were retained. Kompetitive allele
425 specific PCR (KASP) genotyping of clock gene markers (*TaPpd-B1, TaPpd-D1, TaELF3-D1*) and
426 novel SNP markers (*TaPRR73-A1, TaPRR59-B1, TaTOC1-B1, TaLUX-B1*) was completed for
427 the circadian diversity panel. Homoeologue-specific primers for each clock gene marker were
428 designed using PolyMarker[44] (Supplementary Table 6).

429

430 Genotype data for the seven clock gene markers from cultivars in the OzWheat panel plus
431 additional cultivars in this study were used as input for *k*-modes categorical clustering, using only
432 cultivars with complete genotypic data for the seven genes. To choose the value for *k*, the total
433 within-cluster simple-matching distance was calculated and plotted for a range of possible values
434 of *k* (2–10). *k*-modes clustering was performed using the R/klaR package[45]. Chronotypes were
435 visualised in space by multiple correspondence analysis (MCA), performed using the
436 R/FactoMineR package[46]. To estimate the number of dimensions to retain for MCA, *k*-fold cross-
437 validation was performed using the R/missMDA package[47], and the number of dimensions (3) that
438 produced the smallest mean square error of prediction (MSEP) was used for MCA.

439

440 **RNA-sequencing**

441 Wheat seeds of the Australian cultivar Mace were sown in a single growth room in two staggered
442 batches, 28 days apart. Leaves were sampled concurrently when 'mature' plants were at ear
443 emergence (Zadok's stage 51-59) and 'senescent' plants had evident chlorophyll degradation in
444 flag leaves. At dawn (*Zeitgeber* Time 0; ZT0), the growth room was set to continuous light and
445 temperature (20ºC) and whole flag leaves from the primary tiller of four plants were collected
446 every 2 h from ZT45 to ZT91 (48 h). Samples were immediately flash frozen in liquid nitrogen and
447 stored at -80°C.

448

449 Frozen leaf tissue was ground to a fine powder in liquid nitrogen-cooled mortar and pestles.
450 Lysate buffer was added to the tissue (350 µL per 100 mg of tissue) and the mixture was vortexed
451 immediately. RNA was extracted using ISOLATE II RNA Plant Kit (Meridian Bioscience). RNA

452 from two individual leaf samples was equally pooled to provide two replicates for sequencing.
453 Library preparation and RNA-sequencing was performed by a commercial provider (Azenta).
454 Library preparations were constructed using NEBNext Ultra RNA Library Prep Kit for Illumina
455 (New England Biolabs; NEB). Libraries with different indices were multiplexed and sequenced on
456 an Illumina HiSeq platform (Illumina, San Diego, CA). Sequencing was carried out using a 2x150-
457 bp paired-end (PE) configuration. An average of 24 million 150-bp PE reads were generated for
458 each library.
459
460 Reads were filtered for quality and mapped to the *T. aestivum* cv. Mace (PGSBv2.1) genome
461 sequence and annotation using STAR with default parameters[48]. Mapped reads were quantified
462 and normalised using the cuffquant and cuffnorm modules of Cufflinks[49]. Normalised counts
463 (fragments per kilobase transcript per million reads; FPKM) outputted from cuffnorm were used
464 for downstream analyses. Only transcripts that were expressed (i.e. FPKM > 0) at least once in
465 each 24 h period (ZT45-ZT67 and ZT69-ZT91) were retained.
466
467 **Parameterisation of transcript circadian rhythms**
468 The packages BIO_CYCLE[18] and r/MetaCycle[19] were used to estimate rhythmicity and
469 parameterise circadian rhythms of transcripts. BIO_CYCLE was run using default parameters,
470 with minimum and maximum expected period values of 20 and 28 h. MetaCycle incorporates
471 different methods for rhythmicity detection to generate a combined prediction of rhythmicity.
472 JTK_CYCLE and Lomb-Scargle (LS) were selected for integration by MetaCycle. Default settings
473 were maintained for all other parameters. Transcripts with $q < 0.05$ were retained from both
474 BIO_CYCLE and MetaCycle, and the intersection of rhythmic genes from these datasets was
475 used for downstream analyses. All circadian rhythm parameter estimates (period, phase,
476 amplitude, periodicity) presented are derived from BIO_CYCLE. Phase values are adjusted to
477 period (phase = phase(24/period)). The mature-to-senescent change in each of these parameters
478 at the gene level (Δperiod, Δphase and Δamplitude) are used for several analyses. ΔPeriod and
479 Δphase are calculated as the difference between the mature and senescent value of these
480 parameters for a given gene (e.g. Mature period - senescent period). ΔAmplitude is the log ratio
481 of mature and senescent amplitude for a given gene (i.e. log(Mature amplitude: senescent
482 amplitude)).
483
484
485

486 **Gene ontology (GO) term and TF family enrichment analysis**

487 GO terms for the *T. aestivum* cv. Mace (PGSBv2.1) annotation were sourced from Ensembl
488 Plants[50]. r/topGO was used to perform GO enrichment analysis of various gene sets using the
489 'classic' algorithm[51]. Fisher's exact test was selected to compare the enrichment of GO terms in
490 each gene set to a gene universe of 87,493 unique wheat genes with GO term annotations. For
491 enrichment analyses of TF families, Chinese Spring wheat genes annotated as TFs were sourced
492 from https://opendata.earlham.ac.uk/wheat/under_license/toronto/Ramirez-Gonzalez_etal_2018-
493 06025-Transcriptome-Landscape/data/data_tables/[20]. Mace orthologues of each gene were
494 assigned through orthology data available from Ensembl Plants[50]. For enrichment analyses, 2 x
495 2 contingency tables were built for each TF family and analysed with Fisher's exact test (from
496 r/stats). Enrichment analysis of TF families that are only rhythmic in senescent tissue was
497 performed against all rhythmic TFs (rhythmic in senescent, mature or both). Enrichment analysis
498 of differentially rhythmic TFs was performed against all rhythmic TFs (rhythmic in both tissues).

499

500 ***Cis*-regulatory element enrichment**

501 Promoter sequences (1000 bp upstream of the start codon) were obtained from all wheat genes
502 using the 'retrieve sequences' tool from RSAT (Regulatory Sequence Analysis Tools[52]). Promoter
503 sequences were subsetted into groups of interest (e.g. short period genes), and these groups
504 were used as input for *cis*-regulatory element enrichment analysis. For this, promoter sequences
505 from the target set of genes were used as input for RSAT peak-motifs oligo-analysis[53], with all
506 genes that were rhythmic in either mature or senescent flag leaves used as the control set. Peak-
507 motifs settings were kept as default, and significantly enriched oligos with E-value < 0.05 were
508 retained. For each significantly enriched oligo, motif matching was performed with STAMP
509 (Similarity, Tree-building, and Alignment of Motif Profiles[54]) against the PLACE database of plant
510 motifs[55], using default settings. The top match for each oligo (with smallest *p*-value) was retained.

511

512 **Differential expression and differential rhythmicity**

513 LimoRhyde (linear models for rhythmicity, design) was used to test for statistically significant
514 changes in rhythmicity between mature and senescent tissue (differential rhythmicity; DR)[25].
515 LimoRhyde first decomposes *Zeitgeber* Time into sine and cosine with a period of 24 h. Then,
516 transcripts that exhibit DR are identified using a linear model that tests for significant interactions
517 between developmental stage and the time components. LimoRhyde was also used to identify
518 differentially expressed (DE) transcripts. For this, a linear model tests for interactions between
519 developmental stage without interaction of the time components[25]. Code used to perform

LimoRhyde's functions was developed from a vignette from the LimoRhyde GitHub repository (https://github.com/hugheylab/limorhyde). *p*-values were adjusted by the Benjamini-Hochberg procedure with a false discovery rate FDR = 5%[56]. DR and DE genes were assigned using a *q*-value threshold of 0.05. DE genes have log2(fold change) > 1.2 or < -1.2. To allow comparison of circadian rhythm parameters (i.e. period, phase, amplitude), the DR gene set was filtered against the set of genes that are rhythmic in both tissues.

STRING protein-protein network analysis

Protein-protein interactions of DR wheat TFs were analysed using STRING[26]. STRING uses an early genome assembly and annotation for wheat (CSS[57]). CSS gene IDs for the DR gene list were acquired via BLAST searches within STRING, though not all Mace gene annotations had an equivalent locus in the CSS assembly. DR TFs with STRING entries were used to build a protein-protein network in STRING. The network was built using both physical and functional protein interactions, and the minimum weighted interaction score was set to 0.4.

Clustering of oscillator transcript responses

Mace orthologues of putative wheat circadian oscillator genes from Chinese Spring were identified using orthology data from Ensembl Plants[50] (Supplementary Table 2). The list of genes was filtered to include only transcripts that are rhythmic in both mature and senescent tissue. Principal component analysis (PCA) was performed for the 59 clock genes in this list using three variables: mature-to-senescent changes in circadian period, phase, and amplitude (Δperiod, Δphase and Δamplitude). The three PCs from this analysis were used as input for *k*-means clustering. To determine an optimal value of *k*, the ratio of within-cluster sum-of-squares (WCSS) to total sum-of-squares (TSS) was plotted against a range of potential *k* values (1-8). PCA and *k*-means were performed using r/stats.

Acknowledgements

Research was funded by the Research Continuity Scheme from the Faculty of Science, University of Melbourne and the JN Peters Bequest to MJH, and an Alfred Nicholas Fellowship, Melbourne Research Scholarship and Faculty of Science Postgraduate Writing-Up Award to CRB. This research was not funded by the Australian Research Council.

554 **References**

555 1. Gan, S. & Amasino, R. M. Making Sense of Senescence (Molecular Genetic Regulation and
556 Manipulation of Leaf Senescence). *Plant Physiol.* **113**, 313–319 (1997).
557 2. Distelfeld, A., Avni, R. & Fischer, A. M. Senescence, nutrient remobilization, and yield in
558 wheat and barley. *J. Exp. Bot.* **65**, 3783–3798 (2014).
559 3. Chen, L. *et al.* Leaf senescence exhibits stronger climatic responses during warm than
560 during cold autumns. *Nat. Clim. Change* **10**, 777–780 (2020).
561 4. Estiarte, M. & Peñuelas, J. Alteration of the phenology of leaf senescence and fall in winter
562 deciduous species by climate change: effects on nutrient proficiency. *Glob. Change Biol.* **21**,
563 1005–1017 (2015).
564 5. Bucher, S. F. & Römermann, C. The timing of leaf senescence relates to flowering
565 phenology and functional traits in 17 herbaceous species along elevational gradients. *J.*
566 *Ecol.* **109**, 1537–1548 (2021).
567 6. Simmonds, N. W. The relation between yield and protein in cereal grain. *J. Sci. Food Agric.*
568 **67**, 309–315 (1995).
569 7. Christopher, J. T., Christopher, M. J., Borrell, A. K., Fletcher, S. & Chenu, K. Stay-green
570 traits to improve wheat adaptation in well-watered and water-limited environments. *J. Exp.*
571 *Bot.* **67**, 5159–5172 (2016).
572 8. Christopher, M. *et al.* QTL for stay-green traits in wheat in well-watered and water-limited
573 environments. *Field Crops Res.* **217**, 32–44 (2018).
574 9. Alhabbar, Z. *et al.* Associations of NAM-A1 alleles with the onset of senescence and
575 nitrogen use efficiency under Western Australian conditions. *Euphytica* **214**, 180 (2018).
576 10. Sanchez, S. E. & Kay, S. A. The Plant Circadian Clock: From a Simple Timekeeper to a
577 Complex Developmental Manager. *Cold Spring Harb. Perspect. Biol.* **8**, a027748 (2016).
578 11. Bendix, C., Marshall, C. M. & Harmon, F. G. Circadian Clock Genes Universally Control Key
579 Agricultural Traits. *Mol. Plant* **8**, 1135–1152 (2015).
580 12. Zhang, Y. *et al.* Circadian Evening Complex Represses Jasmonate-Induced Leaf
581 Senescence in Arabidopsis. *Mol. Plant* **11**, 326–337 (2018).
582 13. Sakuraba, Y. *et al.* Phytochrome-interacting transcription factors PIF4 and PIF5 induce leaf
583 senescence in Arabidopsis. *Nat. Commun.* **5**, 4636 (2014).
584 14. Kim, H. *et al.* Circadian control of ORE1 by PRR9 positively regulates leaf senescence in
585 Arabidopsis. *Proc. Natl. Acad. Sci.* **115**, 8448–8453 (2018).
586 15. Zhang, Y. *et al.* Circadian Evening Complex Represses Jasmonate-Induced Leaf
587 Senescence in Arabidopsis. *Mol. Plant* **11**, 326–337 (2018).
588 16. Kim, H., Kim, Y., Yeom, M., Lim, J. & Nam, H. G. Age-associated circadian period changes
589 in Arabidopsis leaves. *J. Exp. Bot.* **67**, 2665–2673 (2016).
590 17. Rees, H. *et al.* A high-throughput delayed fluorescence method reveals underlying
591 differences in the control of circadian rhythms in Triticum aestivum and Brassica napus.
592 *Plant Methods* **15**, 51 (2019).
593 18. Agostinelli, F., Ceglia, N., Shahbaba, B., Sassone-Corsi, P. & Baldi, P. What time is it?
594 Deep learning approaches for circadian rhythms. *Bioinformatics* **32**, i8–i17 (2016).
595 19. Wu, G., Anafi, R. C., Hughes, M. E., Kornacker, K. & Hogenesch, J. B. MetaCycle: an
596 integrated R package to evaluate periodicity in large scale data. *Bioinformatics* **32**, 3351–
597 3353 (2016).

598 20. Ramírez-González, R. H. *et al.* The transcriptional landscape of polyploid wheat. *Science*
599 **361**, eaar6089 (2018).
600 21. Nakamichi, N., Kita, M., Ito, S., Yamashino, T. & Mizuno, T. PSEUDO-RESPONSE
601 REGULATORS, PRR9, PRR7 and PRR5, Together Play Essential Roles Close to the
602 Circadian Clock of Arabidopsis thaliana. *Plant Cell Physiol.* **46**, 686–698 (2005).
603 22. Noordally, Z. B. *et al.* Circadian Control of Chloroplast Transcription by a Nuclear-Encoded
604 Timing Signal. *Science* **339**, 1316–1319 (2013).
605 23. Cao, J., Liu, H., Tan, S. & Li, Z. Transcription Factors-Regulated Leaf Senescence: Current
606 Knowledge, Challenges and Approaches. *Int. J. Mol. Sci.* **24**, 9245 (2023).
607 24. Guo, Y. & Gan, S. Leaf senescence: signals, execution, and regulation. *Curr. Top. Dev.*
608 *Biol.* **71**, 83–112 (2005).
609 25. Singer, J. M. & Hughey, J. J. LimoRhyde: A Flexible Approach for Differential Analysis of
610 Rhythmic Transcriptome Data. *J. Biol. Rhythms* **34**, 5–18 (2019).
611 26. Szklarczyk, D. *et al.* The STRING database in 2023: protein-protein association networks
612 and functional enrichment analyses for any sequenced genome of interest. *Nucleic Acids*
613 *Res.* **51**, D638–D646 (2023).
614 27. Harmer, S. L. *et al.* Orchestrated Transcription of Key Pathways in Arabidopsis by the
615 Circadian Clock. *Science* **290**, 2110–2113 (2000).
616 28. Cane, K. *et al.* Ppd-B1 and Ppd-D1 and their effects in southern Australian wheat. *Crop*
617 *Pasture Sci.* **64**, 100–114 (2013).
618 29. Beales, J., Turner, A., Griffiths, S., Snape, J. W. & Laurie, D. A. A Pseudo-Response
619 Regulator is misexpressed in the photoperiod insensitive Ppd-D1a mutant of wheat (Triticum
620 aestivum L.). *Theor. Appl. Genet.* **115**, 721–733 (2007).
621 30. Wittern, L. *et al.* Wheat EARLY FLOWERING 3 affects heading date without disrupting
622 circadian oscillations. *Plant Physiol.* **191**, 1383–1403 (2023).
623 31. Nusinow, D. A. *et al.* The ELF4-ELF3-LUX Complex Links the Circadian Clock to Diurnal
624 Control of Hypocotyl Growth. *Nature* **475**, 398–402 (2011).
625 32. Hicks, K. A. *et al.* Conditional Circadian Dysfunction of the Arabidopsis early-flowering 3
626 Mutant. *Science* **274**, 790–792 (1996).
627 33. Kolmos, E. *et al.* A Reduced-Function Allele Reveals That EARLY FLOWERING3
628 Repressive Action on the Circadian Clock Is Modulated by Phytochrome Signals in
629 Arabidopsis. *Plant Cell* **23**, 3230–3246 (2011).
630 34. Anwer, M. U. *et al.* Natural variation reveals that intracellular distribution of ELF3 protein is
631 associated with function in the circadian clock. *eLife* **3**, e02206 (2014).
632 35. Alvarez, M. A. *et al.* EARLY FLOWERING 3 interactions with PHYTOCHROME B and
633 PHOTOPERIOD1 are critical for the photoperiodic regulation of wheat heading time. *PLOS*
634 *Genet.* **19**, e1010655 (2023).
635 36. Zikhali, M., Wingen, L. U. & Griffiths, S. Delimitation of the Earliness per se D1 (Eps-D1)
636 flowering gene to a subtelomeric chromosomal deletion in bread wheat (Triticum aestivum).
637 *J. Exp. Bot.* **67**, 287–299 (2016).
638 37. Boden, S. A. *et al.* Ppd-1 is a key regulator of inflorescence architecture and paired spikelet
639 development in wheat. *Nat. Plants* **1**, 1–6 (2015).

640 38. Steinfort, U., Trevaskis, B., Fukai, S., Bell, K. L. & Dreccer, M. F. Vernalisation and
641 photoperiod sensitivity in wheat: Impact on canopy development and yield components.
642 *Field Crops Res.* **201**, 108–121 (2017).
643 39. Edelstein, A. D. *et al.* Advanced methods of microscope control using μManager software.
644 *J. Biol. Methods* **1**, e10 (2014).
645 40. Zielinski, T., Moore, A. M., Troup, E., Halliday, K. J. & Millar, A. J. Strengths and Limitations
646 of Period Estimation Methods for Circadian Data. *PLOS ONE* **9**, e96462 (2014).
647 41. Plautz, J. D. *et al.* Quantitative analysis of Drosophila period gene transcription in living
648 animals. *J. Biol. Rhythms* **12**, 204–217 (1997).
649 42. Dupont, F. M., Vensel, W. H., Tanaka, C. K., Hurkman, W. J. & Altenbach, S. B.
650 Deciphering the complexities of the wheat flour proteome using quantitative two-
651 dimensional electrophoresis, three proteases and tandem mass spectrometry. *Proteome*
652 *Sci.* **9**, 10 (2011).
653 43. Hyles, J. E. Genome To Phenome: Diversity For Adaptation And Phenology In Wheat
654 (Triticum aestivum L.). (The University of Sydney, Sydney, Australia, 2021).
655 44. Ramirez-Gonzalez, R. H., Uauy, C. & Caccamo, M. PolyMarker: A fast polyploid primer
656 design pipeline. *Bioinformatics* **31**, 2038–2039 (2015).
657 45. Weihs, C., Ligges, U., Luebke, K. & Raabe, N. klaR Analyzing German Business Cycles. in
658 *Data Analysis and Decision Support* (eds. Baier, D., Decker, R. & Schmidt-Thieme, L.) 335–
659 343 (Springer, Berlin, Heidelberg, 2005). doi:10.1007/3-540-28397-8_36.
660 46. Lê, S., Josse, J. & Husson, F. FactoMineR: An R Package for Multivariate Analysis. *J. Stat.*
661 *Softw.* **25**, 1–18 (2008).
662 47. Josse, J. & Husson, F. missMDA: A Package for Handling Missing Values in Multivariate
663 Data Analysis. *J. Stat. Softw.* **70**, 1–31 (2016).
664 48. Dobin, A. *et al.* STAR: ultrafast universal RNA-seq aligner. *Bioinformatics* **29**, 15–21 (2013).
665 49. Trapnell, C. *et al.* Transcript assembly and quantification by RNA-Seq reveals unannotated
666 transcripts and isoform switching during cell differentiation. *Nat. Biotechnol.* **28**, 511–515
667 (2010).
668 50. Cunningham, F. *et al.* Ensembl 2022. *Nucleic Acids Res.* **50**, D988–D995 (2022).
669 51. Alexa, A., Rahnenführer, J. & Lengauer, T. Improved scoring of functional groups from gene
670 expression data by decorrelating GO graph structure. *Bioinformatics* **22**, 1600–1607 (2006).
671 52. Nguyen, N. T. T. *et al.* RSAT 2018: regulatory sequence analysis tools 20th anniversary.
672 *Nucleic Acids Res.* **46**, W209–W214 (2018).
673 53. Thomas-Chollier, M. *et al.* RSAT peak-motifs: motif analysis in full-size ChIP-seq datasets.
674 *Nucleic Acids Res.* **40**, e31 (2012).
675 54. Mahony, S. & Benos, P. V. STAMP: a web tool for exploring DNA-binding motif similarities.
676 *Nucleic Acids Res.* **35**, W253–W258 (2007).
677 55. Higo, K., Ugawa, Y., Iwamoto, M. & Higo, H. PLACE: A database of plant cis -acting
678 regulatory DNA elements. *Nucleic Acids Res.* **26**, 358–359 (1998).
679 56. Benjamini, Y. & Hochberg, Y. Controlling the False Discovery Rate: A Practical and
680 Powerful Approach to Multiple Testing. *J. R. Stat. Soc. Ser. B Methodol.* **57**, 289–300
681 (1995).

682 57. International Wheat Genome Sequencing Consortium (IWGSC). A chromosome-based draft
683 sequence of the hexaploid bread wheat (Triticum aestivum) genome. *Science* **345**, 1251788
684 (2014).
685
686